α_2 Macroglobulin Receptor/Ldl Receptor-related Protein(Lrp)-dependent Internalization of the Urokinase Receptor

Massimo Conese,* Anders Nykjær,‡ Claus M. Petersen,‡ Ottavio Cremona,‖ Ruggero Pardi,**
Peter A. Andreasen,¶ Jørgen Gliemann,‡ Erik I. Christensen,§ and Francesco Blasi*

*Molecular Genetics Unit, Dipartimento di Ricerca Biologica e Tecnologica, H.S. Raffaele Scientific Institute, and Dipartimento di Genetica e Biologia dei Microrganismi, Università di Milano; Departments of‡Medical Biochemistry, §Cell Biology, and ¶Molecular Biology, University of Aarhus, Aarhus 8000, Denmark;‖Dipartimento di Scienze Mediche, Università di Torino, Novara, Italy; and **Clinical Immunology Unit, DIBIT, H.S. Raffaele Scientific Institute, via Olgettina 60, 20132 Milano, Italy

Abstract. The GPI-anchored urokinase plasminogen activator receptor (uPAR) does not internalize free urokinase (uPA). On the contrary, uPAR-bound complexes of uPA with its serpin inhibitors PAI-1 (plasminogen activator inhibitor type-1) or PN-1 (protease nexin-1) are readily internalized in several cell types. Here we address the question whether uPAR is internalized as well upon binding of uPA-serpin complexes. Both LB6 clone 19 cells, a mouse cell line transfected with the human uPAR cDNA, and the human U937 monocytic cell line, express in addition to uPAR also the endocytic α_2-macroglobulin receptor/low density lipoprotein receptor–related protein (LRP/α_2-MR) which is required to internalize uPAR-bound uPA-PAI-1 and uPA-PN-1 complexes. Downregulation of cell surface uPAR molecules in U937 cells was detected by cytofluorimetric analysis after uPA-PAI-1 and uPA-PN-1 incubation for 30 min at 37°C; this effect was blocked by preincubation with the ligand of LRP/α_2-MR, RAP (LRP/α_2-MR-associated protein), known to block the binding of the uPA complexes to LRP/α_2-MR. Downregulation correlated in time with the intracellular appearance of uPAR as assessed by confocal microscopy and immuno-electron microscopy. After 30 min incubation with uPA-PAI-1 or uPA-PN-1 (but not with free uPA), confocal microscopy showed that uPAR staining in permeabilized LB6 clone 19 cells moved from a mostly surface associated to a largely perinuclear position. This effect was inhibited by the LRP/α_2-MR RAP. Perinuclear uPAR did not represent newly synthesized nor a preexisting intracellular pool of uPAR, since this fluorescence pattern was not modified by treatment with the protein synthesis inhibitor cycloheximide, and since in LB6 clone 19 cells all of uPAR was expressed on the cell surface. Immuno-electron microscopy confirmed the plasma membrane to intracellular translocation of uPAR, and its dependence on LRP/α_2-MR in LB6 clone 19 cells only after binding to the uPA-PAI-1 complex. After 30 min incubation at 37°C with uPA-PAI-1, 93% of the specific immunogold particles were present in cytoplasmic vacuoles vs 17.6% in the case of DFP-uPA. We conclude therefore that in the process of uPA-serpin internalization, uPAR itself is internalized, and that internalization requires the LRP/α_2-MR.

IN processes like cellular invasion and cell migration extracellular proteolytic activities are localized at the moving edges of the cells. Urokinase plasminogen activator (uPA)[1] is a cell surface protease that regulates cell migration and invasiveness either through a focal and transient activation of plasminogen, hepatocyte growth factor, and TGF-β1 or through a direct effect on mitogenesis, cell adhesion, and chemotaxis (for review see Fazioli and Blasi, 1994). The cell surface association of uPA depends on the high affinity interaction with a specific receptor (uPAR), via its growth factor domain (Vassalli et al., 1985; Stoppelli et al., 1985; Appella et al., 1987). The importance of uPA and uPAR in tumor invasion is underlined by the possibility to block basement membrane degradation, cancer cell invasion, and experimental metastasis

1. *Abbreviations used in this paper:* ATF, amino-terminal fragment of uPA; GPI, glycosyl-phosphatidylinositol; LRP/α_2-MR, α_2-macroglobulin receptor/low density lipoprotein receptor–related protein; PAI-1, plasminogen activator inhibitor type-1; PN-1, protease-nexin 1; pro-uPA, pro-urokinase; RAP, α_2-macroglobulin receptor/low density lipoprotein receptor–associated protein; uPA, urokinase type plasminogen activator; DFP-uPA, diisopropyl-fluorophosphate–inhibited uPA; uPAR, urokinase-type plasminogen activator receptor.

with inhibitors of uPA and antagonists of its surface localization (Bergman et al., 1986; Ossowski and Reich, 1983; Hearing et al., 1988; Ossowski, 1988; Ossowski et al., 1991; Quax et al., 1991; Crowley et al., 1993; Kook et al., 1994; Kobayashi et al., 1994). The activity of uPA is controlled by specific endogenous inhibitors (PAI-1, PAI-2, and PN-1) belonging to the superfamily of serpins (serine protease inhibitors) (Huber and Carrell, 1989; Potempa et al., 1994), which can react with uPAR-bound uPA and inhibit cell surface uPA enzymatic activity (Cubellis et al., 1989; Kirchheimer and Remold, 1989; Ellis et al., 1989; Estreicher et al., 1990).

When active uPA is bound to the receptor, it is not internalized but remains at the cell surface (Vassalli et al., 1985; Stoppelli et al., 1985; Cubellis et al., 1986; Stoppelli et al., 1986). When, however, receptor-bound uPA is complexed to PAI-1, PAI-2, or PN-1, the complex is internalized and degraded (Cubellis et al., 1990; Jensen et al., 1990; Estreicher et al., 1990; Conese et al., 1994). Binding to uPAR is required for internalization and degradation of uPA-serpin complex (Olson et al., 1992; Nykjær et al., 1992; Conese et al., 1994). However, it has been recently shown that a *trans*-membrane receptor belonging to the LDL-receptor family, namely the α_2-macroglobulin receptor/low density lipoprotein receptor–related protein (LRP/α_2-MR) (or the epithelial glycoprotein-330, gp330, in kidney) is also required for uPA:serpins internalization and degradation (Nykjær et al., 1992; Herz et al., 1992; Orth et al., 1992; Moestrup et al., 1993a; Li et al., 1994).

LRP/α_2-MR is a multiligand receptor that binds α_2-macroglobulin:proteinase complexes (Moestrup et al., 1990), tissue-plasminogen activator (tPA) and tPA–PAI-1 complexes (Orth et al., 1992), uPA–PAI-1 and uPA–PN-1 complexes (Nykjær et al., 1992; Conese et al., 1994), pro-uPA (Kounnas et al., 1993; Nykjær et al., 1994a), apolipoprotein E-enriched β-migrating very low density lipoprotein (Kowal et al., 1990), lipoprotein lipase (Beisigel et al., 1991; Nykjær et al., 1994b), lactoferrin (Willnow et al., 1992), *Pseudomonas aeruginosa* exotoxin A (Kounnas et al., 1992), the plant type I ribosome-inactivating protein saporin (SAP) and its conjugate with uPA (Conese et al., 1995), and a 39–40-kD receptor-associated protein (RAP) (Jensen et al., 1989; Ashcom et al., 1990; Strickland et al., 1991). uPA-serpin degradation in various cell types can be inhibited by RAP and by antibodies against the LRP/α_2-MR (Nykjær et al., 1992; Willnow et al., 1992; Herz et al., 1992; Kounnas et al., 1993; Conese et al., 1994). The uPA-PAI-1 complex binds to LRP/α_2-MR through sites localized in PAI-1, as well as in both the serine protease domain and the A-chain of uPA, indicating the involvement of several independent binding contacts with LRP/α_2-MR (Nykjær et al., 1994a).

The various steps in uPA-serpin internalization and degradation are still poorly understood. uPA-PAI-1 internalization and lysosomal accumulation can be followed by immunofluorescence and by electron microscopy (Jensen et al., 1990; Olson et al., 1992), and it is known that LRP/α_2-MR is itself internalized (Moestrup et al., 1990; Hopkins et al., 1994). However, whether uPAR is also internalized along with the uPA-serpin and LRP/α_2-MR is still unknown. In this paper we directly show that binding of uPA-serpins to the cells induces internalization of uPAR.

Materials and Methods

Reagents

Two chain uPA was obtained from Lepetit SpA, courtesy of Dr. M. L. Nolli, and recombinant pro-uPA from Dr. Paolo Sarmientos (Primm, Milano). DFP-uPA (uPA inhibited with diisopropyl-fluorophosphate) was prepared as previously described (Nykjær et al., 1990). Anti-uPAR monoclonal antibody R2 was purified on a protein G Sepharose column using a commercial kit (mAbTrap™ G, Pharmacia LKB, Sweden) from hybridoma cell culture supernatant and was donated by Drs. E. Rønne and G. Høyer-Hansen (Finsen Laboratory, Rigshospitalet, Copenhagen) (Rønne et al., 1991). Recombinant active PAI-1 (Sherman et al., 1992) and recombinant PN-1 (PN-1) were generously donated by Dr. David Ginsburg (Howard Hughes Medical Institute, Ann Arbor, MI) and Dr. Randy Scott (Incyte Co., Palo Alto, CA), respectively. Recombinant 39 kD RAP and rabbit antiserum raised against a recombinant α-chain fragment of LRP/α_2-MR (amino acids 2500-2922) have been described before (Nykjær et al., 1992, 1994a). Purified LRP/α_2-MR and gp330 were prepared as described previously (Moestrup and Gliemann, 1991; Moestrup et al., 1993a). Benzamidine Sepharose 6B was from Pharmacia LKB Biotechnology (Piscataway, NJ); dimethyl-diphenylpolysiloxane and cycloheximide were from Sigma Chem. Co (St. Louis, MO). The cross-linking reagent disuccinimidyl-suberate was obtained from Pierce Chem. Co. (Rockford, IL). Phosphatidylinositol-specific phospholipase C (PI-PLC) from *B. cereus* was from Boehringer Mannheim Gmbh (Penzberg, Germany).

Cell Lines and Cell Cultures

Growth conditions for the human monocyte-like U937 cells and for the murine LB6 clone 19 cells, a mouse cell line expressing the human uPA-receptor, have been previously described (Picone et al., 1989; Roldan et al., 1990).

The assays for ligand binding, internalization, and degradation for both U937 and LB6 clone 19 cells have been previously described (Olson et al., 1992; Conese et al., 1994).

Iodinations

Iodination of uPA, ATF, and RAP with Iodogen (Pierce Chem. Co.) has been described (Behrendt et al., 1990; Nykjær et al., 1992). Specific activities of the proteins ranged between 2.5 and 7.5 × 10^5 cpm/pmol. Enzymatically active iodinated uPA was purified by affinity chromatography on benzamidine Sepharose 6B (Holmberg et al., 1976).

Formation of uPA-serpin Complexes

uPA–PAI-1 complexes were formed combining benzamidine-Sepharose purified ^{125}I- or unlabeled uPA and a 50-fold molar excess of PAI-1 at room temperature for 2 h. The inhibitor:uPA ratio was experimentally determined to convert over 90% of the uPA to the complex form as determined by SDS-PAGE analysis (not shown). uPA–PN-1 was formed under identical conditions, as previously described (Conese et al., 1994).

Cytofluorimetric Analysis

Acid washed–U937 cells (10^6) were incubated with 1 nM uPA, uPA–PAI-1, or uPA-PN-1 complexes for 2 h at 4°C eventually followed by 30 min at 37°C. Cells were washed twice with PBS, and incubated in 0.1 ml PBS and 30 μg/ml of the uPAR-specific monoclonal antibody (Rønne et al., 1991) R2 for 30 min at 4°C. Cells were then washed twice with PBS and resuspended in PBS containing a 1:50 dilution of fluorescein-conjugated antibody against mouse IgG (Dakopatts, Copenhagen, Denmark). After 30 min at 4°C, cells were washed twice and analyzed by flow cytofluorimetry with a FACScan apparatus (Becton Dickinson, San Jose, CA). To express the data, the cell number was plotted against the log of the mean fluorescence intensity. About 5,000 cells were measured at each determination. The negative control was obtained incubating the cells in the absence of the primary antibody.

Confocal Immunofluorescence Microscopy

For confocal microscopy, 0.2 × 10^6 LB6 clone 19 cells were plated onto 24-well Costar plates containing 1.4 cm² round glass coverslips. Coverslip-

attached cells were fixed in 3% formaldehyde (freshly prepared from paraformaldehyde) in PBS, pH 7.6 containing 2% sucrose for 10 min at 4°C. Coverslips were soaked, after fixation, for 1 min in ice-cold Hepes-Triton X-100 buffer (20 mM Hepes, pH 7.4, 3 mM MgCl$_2$ and 0.5% Triton X-100) to obtain permeabilization. Monoclonal anti-uPAR antibody R2 was used at 15 μg/mL in TBS-0.2% BSA. As secondary antibody, we used a goat-anti–mouse rhodamine-conjugated IgG F(ab') 2 fragment (Protos Immunoresearch, San Francisco, CA) diluted 1:200 in TBS-0.2% BSA. Coverslips were then mounted in 20% Mowiol 4-88 in TBS (HOECHST AG, Frankfurt, Germany). Observations were carried out on a Sarastro 2000 confocal laser scanning system (Molecular Dynamics, Sunnyvale, CA) equipped with a two wavelength Argon ion laser (488 and 514 nm) and with a Zeiss Axioskop fluorescence microscope. The objectives used were a plan-apochromatic 63×/1.4 and a plan-apochromatic 100×/1.3 (Carl Zeiss). Optical sections of 0.29 μm thickness were saved as 512 × 512 pixel images at 8 bit resolution (256 gray levels), and then processed as TIFF files on a Silicon graphics workstation. Images were printed on photographic quality paper using a sublimation ink printer (Mitsubishi Electric Corporation, Tokyo, Japan).

Electron Microscopy

LB6 clone 19 cells (5 × 10⁶) were incubated under four different conditions: (a) for 2 h with 100 nM uPA–PAI-1 at 0°C, washed, and then fixed; (b) preincubated for 2 h with 100 nM uPA–PAI-1 at 0°C, washed and chased for 30 min at 37°C, fixed; (c) preincubated for 30 min at 0°C with 400 nM RAP, and then for 2 h with 100 nM uPA–PAI-1 at 0°C together with RAP, washed and chased in the presence of 400 nM RAP for 30 min at 37°C and finally fixed; (d) preincubated for 2 h with 100 nM DFP-uPA at 0°C, chased for 30 min at 37°C, and then fixed. In all cases, incubation mixtures contained 5 mM methylamine. The cells were fixed with 0.1% glutaraldehyde and 2% formaldehyde in 0.1 M sodium cacodylate buffer, pH 7.2, for 1 h and subsequently postfixed for up to 18 h in 2% formaldehyde in the same buffer. The cells were then infiltrated with 2.3 M sucrose containing 2% formaldehyde for 30 min and frozen in liquid nitrogen. Ultrathin cryosections, 70–90 μm, were obtained with a FCS Reichert Ultracut S cryoultramicrotome at about −100°C and collected on 300 mesh Ni grids. The sections were incubated overnight at 4°C with the mouse monoclonal anti-uPAR antibody R2, 16–40 μg/ml or with a polyclonal affinity-purified rabbit anti-uPAR antibody (2.5 μg/ml) and subsequently with 10-nm goat anti-mouse-gold or goat anti-rabbit-gold (BioCell, Cardiff, UK) at 4°C for 2 h. The sections were finally contrasted with methyl cellulose containing 0.3% uranylacetate (Tokuyasu, 1978; Griffiths et al., 1984) and studied in a Philips EM208 or a Philips CM100 electron microscope. Controls, incubated with nonspecific monoclonal antibody, protein A affinity purified rabbit immunoglobulin, preabsorbed polyclonal rabbit anti-uPAR immunoglobulin or without primary antibody showed no specific labeling at all.

The immunogold distribution over the cells, using the polyclonal affinity-purified rabbit anti-uPAR antibody, was determined quantitatively as follows. Approximately 25 electron micrographs were taken at random, but including as much cytoplasm and cell surface as possible from each of the four groups at a primary magnification of 15,500, and then enlarged 3×. Gold-particles were counted over the plasma membrane and over cytoplasmic vacuoles. The cytoplasmic areas analyzed in the four groups, as determined by point counting, were essentially identical (311 μm² for a, 423 for b, 379 for c, and 420 for d). The total number of gold particles counted was 8,149. The background labeling which was determined in the four groups by counting gold particles over nuclei was extremely low, ranging from 0.2–0.4 gold particles/μm².

Release of uPAR by PI-PLC and Cross-Linking to ¹²⁵I-ATF

LB6 clone 19 cells (0.2 × 10⁶/well) were incubated with serum-free medium or with medium supplemented with phosphatidylinositol-specific phospholipase C (PI-PLC) (10 U/ml) for 15 min at 37°C. At the end of the incubation, the supernatant was recovered and the pelleted cells were extracted in lysis buffer (0.1 M Tris-Cl, pH 8.1, 10 mM EDTA, 1% Triton X-100, and 1% aprotinin). Cell extracts or supernatants were cleared at 15,000 g for 10 min at 4°C and tested for uPAR by cross-linking to ¹²⁵I-ATF (60,000 cpm), using 1 mM disuccinimidyl suberate, as previously described (Behrendt et al., 1990). The samples were analyzed by SDS-PAGE (12%) gel electrophoresis (Laemmli, 1970) under nonreducing conditions. The

specificity of the ¹²⁵I-ATF–uPAR conjugate was demonstrated by competition with unlabeled free uPA.

Ligand- and Immuno-Blotting Procedures

For ligand blotting, purified LRP/α₂-MR or detergent phase separated membrane fractions were run in 4–16% SDS-PAGE under nonreducing conditions, electroblotted to PVDF membranes (Immobilon, Millipore) and blocked for 2 h at 20°C in binding buffer (140 mM NaCl, 10 mM Hepes, 2 mM CaCl₂, 1 mM MgCl₂, pH 7.8) containing 2% defatted milk powder. The filters were then incubated for 16 h at 4°C in the presence of 50 pM iodinated ligands in binding buffer supplemented with 0.5% BSA, washed three times, and autoradiographed for 12–18 h.

Immuno-blotting with a rabbit-antiserum raised against a recombinant fragment of the α-chain of LRP/α₂-MR, was performed as described previously (Nykjær et al., 1994a).

Results

LRP/α₂-MR Dependence of the Internalization of the uPA-Serpin Complexes in U937 and LB6 Clone 19 Cells

Efficient internalization of uPA–PAI-1 requires the participation of both LRP/α₂-MR (Strickland et al., 1991; Nykjær et al., 1992; Herz et al., 1992; Willnow et al., 1992; Moestrup et al., 1993b; Conese et al., 1994) and uPAR (Olson et al., 1992; Conese et al., 1994). We first tested for the presence of LRP/α₂-MR in LB6 clone 19 cells, a murine cell line transfected with human uPAR cDNA (Roldan et al., 1990). Triton X-114 extracts of LB6 clone 19 cells were phase separated and analyzed for the presence of LRP/α₂-MR and uPAR in both the water and the detergent phases. Purified LRP/α₂-MR and gp330 were used as positive controls in the identification. Cell extracts in Triton X-114 were phase separated and the two phases analyzed, by ligand blotting procedures, for binding to ¹²⁵I-uPA–PAI-1, ¹²⁵I-RAP and to anti-LRP/α₂-MR antibodies. The following data (Fig. 1) show that LB6 clone 19 cells contain, in addition to uPAR, also LRP/α₂-MR. In the water soluble extract, ¹²⁵I-uPA–PAI-1 bound to a slowly migrating band comigrating with authentic LRP/α₂-MR; however, in the detergent-soluble extract, it bound to a different faster migrating band (first panel). The latter band corresponds to uPAR on the basis of comigration with authentic uPAR (not shown) and several previously published criteria (Plough et al., 1991; Behrendt et al., 1990; Conese et al., 1994). On the other hand, ¹²⁵I-RAP bound only to the LRP/α₂-MR band in the water-phase, and did not bind to any protein present in the detergent phase (Fig. 1, second panel). The binding of ¹²⁵I-uPA–PAI-1 to LRP/α₂-MR–comigrating band in the water extract was competed for by unlabeled RAP (Fig. 1, fourth panel), supporting the identification of this band as LRP/α₂-MR. Finally, the LRP/α₂-MR band in the water phase was recognized by specific anti-LRP/α₂-MR antibodies (third panel). We conclude, therefore, that LB6 clone 19 cells contain, in addition to uPAR, also LRP/α₂-MR. The presence of both these receptors on U937 cells was previously reported (Conese et al., 1995).

We next tested whether internalization and degradation of uPA–PAI-1 in LB6 clone 19 cells were also dependent on the LRP/α₂-MR. RAP and a soluble LRP/α₂-MR, reagents which interfere with the binding of all ligands to cellular LRP/α₂-MR, did not inhibit binding of uPA, uPA–
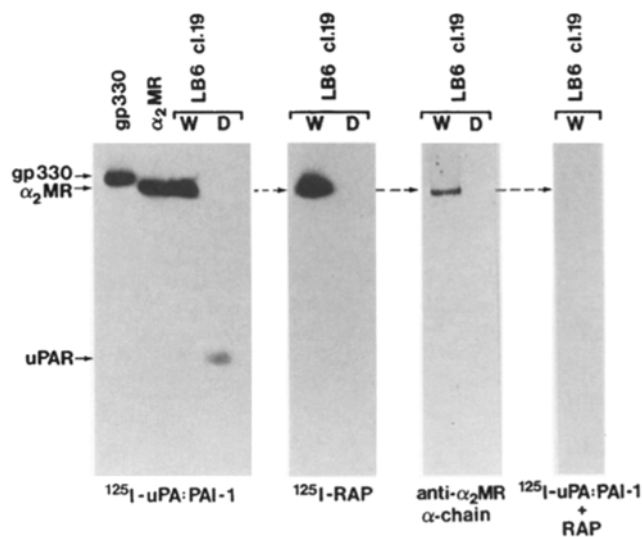
Figure 1. Ligand blot analysis shows that LB6 clone 19 cells contain LRP/α_2-MR. 0.25 μg purified gp330 or LRP/α_2-MR and detergent (D) and water (W) phases from extracts in Triton X-114 prepared from 5 ×10⁶ LB6 clone 19 cells, were applied to 4–16% SDS-PAGE, electroblotted to PDVF membranes, blocked, and incubated for 16 h at 4°C with the reagents indicated at the bottom of each lane at the following concentrations: 50 pM ¹²⁵I-uPA-PAI-1 in the absence or presence of 400 nM RAP; 50 pM ¹²⁵I-RAP or 1:1,000 dilution of LRP/α_2-MR antiserum. After washing the membranes, bound radioactivity was visualized by autoradiography while anti-LRP/α_2-MR antibodies were detected by a peroxidase-coupled anti-rabbit antibody (see Materials and Methods).

PAI-1 and uPA–PN-1 complexes to neither of the two cell lines LB6 clone 19 and U937 cells (data not shown), in agreement with published data (Nykjær et al., 1992; Olson et al., 1992; Conese et al., 1994). However, internalization and degradation of ¹²⁵I-uPA–PAI-1 in LB6 clone 19 cells were inhibited by these two reagents. As shown in Fig. 2 A, the amount of internalized ¹²⁵I-uPA–PAI-1 was maximal at 30 min of incubation and decreased thereafter. On the contrary, degradation of ¹²⁵I-uPA–PAI-1 reached saturation at about 60 min (Fig. 2 B). Both internalization and degradation of ¹²⁵I-uPA–PAI-1 were strongly decreased when the experiment was carried out in the presence of RAP or of the soluble LRP/α_2-MR. The same results were obtained with U937 cells and for uPA–PN-1 complexes (not shown). The high background of internalization at time zero is a phenomenon regularly observed even in the presence of noninternalized ligands of uPAR (Cubellis et al., 1990), and is not accompanied by degradation (which is in fact null at this time, Fig. 2 B), thus probably representing an artifact due to the temperature shift (see also another experiment, in Fig. 6). The overall results of this experiment are in line with previous data on other cell lines and with the hypothesis that the uPA-serpin complexes first bind to cell surface uPAR and subsequently are transported intracellularly via the LRP/α_2-MR (Nykjær et al., 1992; Conese et al., 1994).

From these data and from those in the literature (Nykjær et al., 1992; Herz et al., 1992; Kounnas et al., 1993; Conese et al., 1994), we conclude that in U937 and LB6 clone 19 cells uPA-serpin internalization occurs in three steps: a first
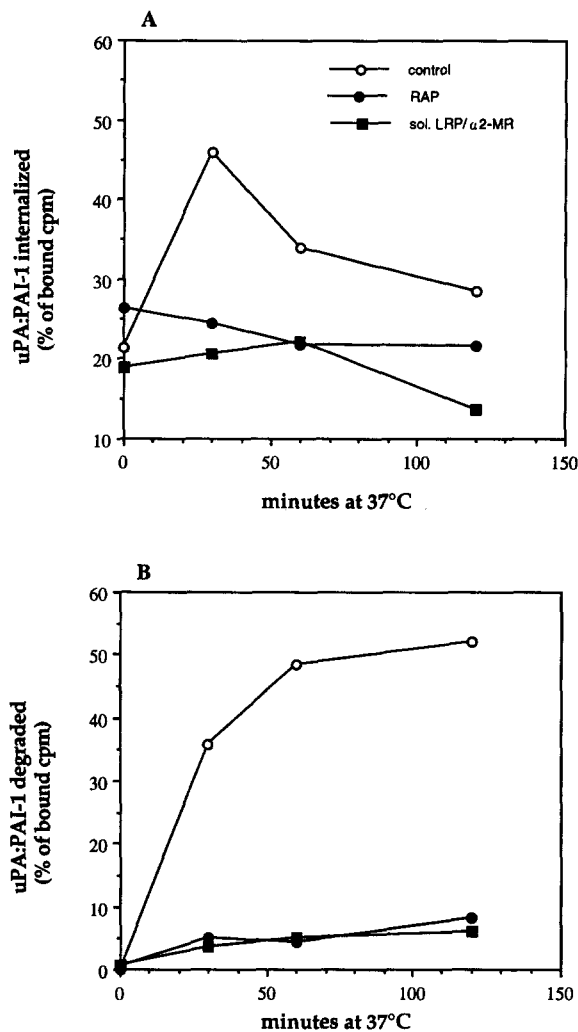

Figure 2. RAP and soluble LRP/α_2-MR inhibit ¹²⁵I-uPA–PAI-1 internalization and degradation in LB6 clone 19 cells. LB6 clone 19 (0.2 × 10⁶/well) were incubated with 100,000 cpm ¹²⁵I-uPA–PAI-1 (1 nM, 9,000 cpm/ng) for 2 h at 4°C, and then transferred at 37°C for various time intervals in the absence (open circles) or in the presence of 200 nM RAP (closed circles) or 200 nM soluble LRP/α_2-MR (closed squares). Internalized ligand (i.e., radioactivity remaining in the cell pellet after acid washing) (A) and degraded ligand (trichloroacetic acid–soluble radioactivity in the supernatant) (B) were determined as described in the Materials and Methods section, and expressed as a percent of total radioactivity bound at 4°C. Nonspecific binding was determined in the presence of 200 nM pro-uPA and substracted. Specifically bound radioactivity at 4°C was 2.6 fmol/well (2.4 and 2.8 in the two experiments). Data are the average of two experiments in duplicate.

step of binding to uPAR, a second step which must include the interaction of uPAR-bound uPA-serpin with the LRP/α_2-MR, and a third step leading to internalization of the complexes.

uPA–PAI-1-dependent Internalization of uPAR in U937 and LB6 Clone 19 Cells. Requirement for LRP/α_2-MR

We have tested whether the internalization of the uPA-serpin complexes is accompanied by the internalization of uPAR. If uPAR is internalized, its expression on the cell

surface is expected to be reduced during the internalization of uPA–PAI-1 or uPA–PN-1. Therefore, the presence of uPAR on the cell surface of human U937 cells was studied by FACS analysis using anti-uPAR monoclonal antibodies that can be followed by cytofluorimetry with a fluorescent anti-mouse antibody. As shown in Fig. 3 A, specific uPAR fluorescence was measured with antibody R2 on U937 cells incubated at 4°C for 120 min with 1 nM uPA–PAI-1 or free uPA. In control experiments (not shown), it was established that binding of uPA, uPA–PAI-1, or uPA–PN-1 did not interfere with the recognition of uPAR by the antibody R2 by the cytofluorimetric technique, in agreement with the domain specificity of this antibody (Rønne et al., 1991). The same level of fluorescence was measured when cells were incubated with uPA or uPA–PAI-1 (Fig. 3 A). When the cells were allowed to incubate for additional 30 min at 37°C, a decrease in fluorescence was observed with uPA–PAI-1, as evidenced by a leftward shift in the mean fluorescence peak, but not with uPA (Fig. 3 A). A similar downregulation was observed with uPA–PN-1 complexes (not shown). To test whether the reduction in uPAR-specific fluorescence was really correlated to uPA–PAI-1 or uPA–PN-1 internalization, we repeated the experiment testing also the effect of the LRP/α_2-MR ligand RAP. As shown in Fig. 3 B, the decrease in uPAR-fluorescence observed after incubation of U937 cells with both uPA-PAI-1 and uPA–PN-1 at 37°C was prevented by the presence of RAP. These results therefore show that in U937 cells a downregulation of cell-surface uPAR occurs during uPA–PAI-1 and uPA–PN-1 internalization, and suggest that this process may require LRP/α_2-MR.

To better examine internalization of uPAR, we used confocal epifluorescence microscopy. LB6 clone 19 cells were incubated with uPA or uPA–PAI-1 for 120 min at 4°C, washed and incubated at 37°C in the absence of ligand for an additional 30 min. At the end of the 4° or 37°C incubation, the cells were permeabilized, fixed, and stained with the anti-uPAR mAb R2 (see Materials and Methods). Upon incubation at 4°C with either uPA (Fig. 4 a) or uPA–PAI-1, (Fig. 4, b–d), staining of uPAR was visible largely at the periphery of the cells, most strongly at the cell contours. Treatment of the cells with cycloheximide before the incubation with uPA or uPA–PAI-1 did not drastically change this picture.

We next followed uPAR immunofluorescence during uPA-PAI-1 internalization, i.e., analyzing cells after a shift to 37°C for 30 min, a time providing maximal intracellular enrichment of uPA–PAI-1 (see f.e., Fig. 1). As shown in Fig. 4, e–g, under these conditions uPAR was detected inside the cells, largely in the perinuclear region. Perinuclear location was not exclusive, however, since staining was still observed at the periphery. The results suggest that uPAR was at least in part internalized in uPA–PAI-1-challenged LB6 clone 19 cells during the 37°C incubation. Similar results were obtained with the uPA–PN-1 complex, whereas no perinuclear staining was observed with free uPA (data not shown). The persistence of cell surface uPAR under the internalization conditions is explained by the use of non-saturating conditions of ligands (1 nM). Importantly, the presence of the LRP/α_2-MR ligand RAP throughout the experiment totally prevented the intracellular localization (Fig. 4 h). These results overall strongly suggest that in the
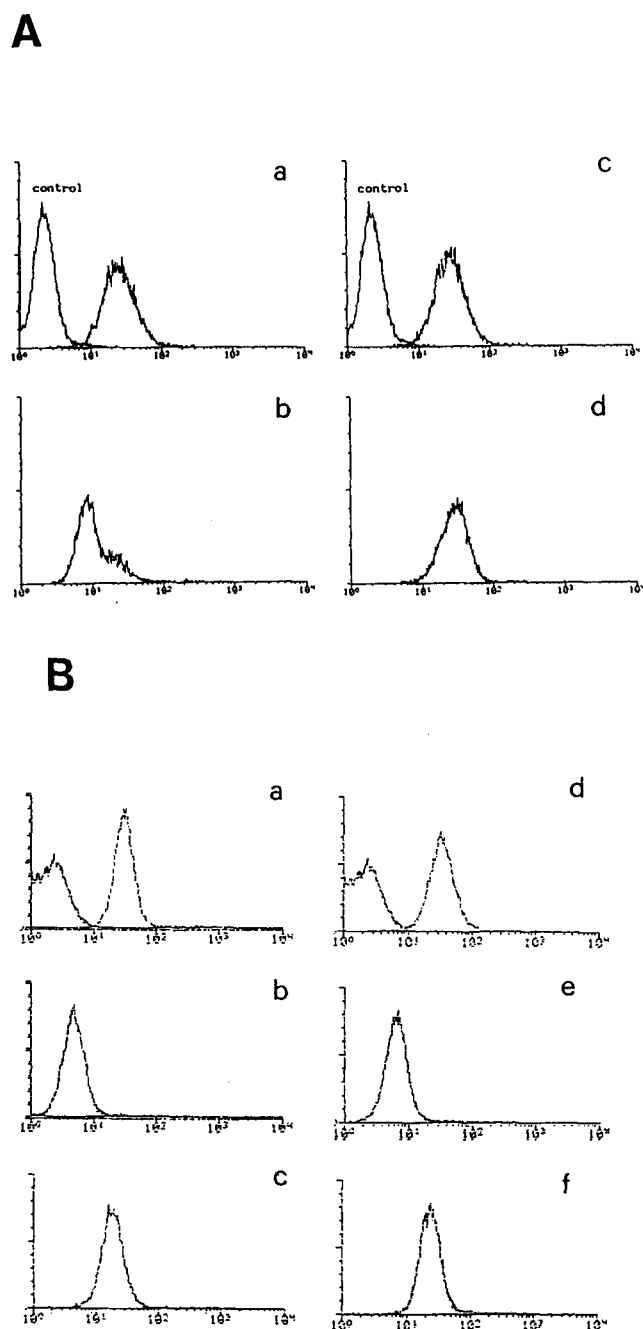

Figure 3. Cytofluorimetric analysis of uPAR downregulation during uPA–PAI-1 and uPA–PN-1 internalization in U937 cells: LRP/α_2-MR dependence. In all graphs, the abscissae show the mean fluorescence intensity (log scale), while the ordinates represent the channel number (linear scale), i.e., the number of cells. (A) The left panels (a and b) refers to cells challenged with uPA–PAI-1, the right panels (c and d) to cells challenged with uPA (1 nM in both cases). Control peak in a refers to cells treated only with the fluorescein-conjugated antibody. Monoclonal anti-uPAR antibody R2 was used for the analysis. Shown in a and c is the cytofluorimetric analysis of cells incubated only at 4°C; in b and d the cells were incubated with the ligand at 4°C for 120 min, and then exposed to 37°C for 30 min. (B) The cells were incubated with 1 nM uPA-PAI-1 (a, b, and c) or uPA–PN-1 (d, e, and f) for 120 min at 4°C in the absence (a, b, d, and e) or in the presence of 200 nM RAP (c and f), and then either maintained at 4°C (a and d) or incubated for 30 min at 37°C in the absence (b and e) or in the presence of 200 nM RAP (c and f). Control peak in panel a refers to cells treated only with the fluorescein-conjugated antibody.
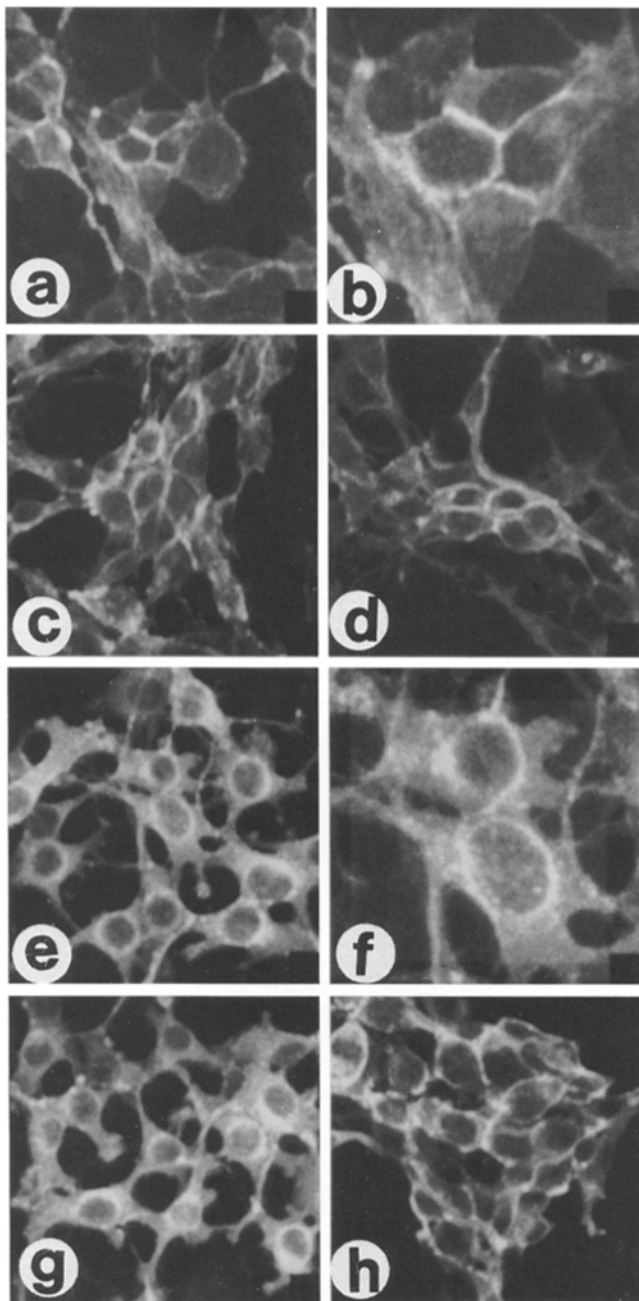
presence of uPA–PAI-1 at 37°C uPAR is internalized and that internalization requires LRP/α_2-MR.

In a separate experiment carried out under the same conditions, the specific immunofluorescence of LB6 clone 19 cells challenged with uPA–PAI-1 at 4°C was analyzed at different planes of focus from apical to basal (confocal sectioning), and the image of a sagittal section computer-reconstructed from optical sections of 0.29 μm thickness (data not shown). The data of the different sections were saved and processed to reconstruct a sagittal projection which showed that the interior of the cell was mostly devoid of specific staining with the strongest staining present at the cell contours. When, however, the sagittal section was reconstructed from cells exposed to uPA–PAI-1 at 4°C for 2 h, but then chased at 37° for 30 min, the interior of the cell was now clearly strongly positive for uPAR (not shown).

Immunofluorescence of LB6 clone 19 cells shows a slight, but visible background (see Fig. 4). This background could interfere with the interpretation of the data since the perinuclear location might also indicate the presence of biosynthetic uPAR. The internalization experiment performing under conditions in which protein synthesis is blocked should result in the inhibition of that part of the perinuclear staining due to biosynthetic uPAR. We first studied the effect of cycloheximide on uPA–PAI-1 uptake and
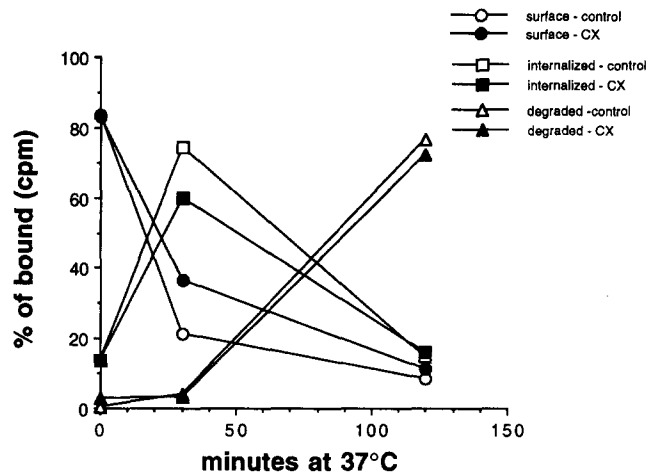

Figure 4. Confocal immunofluorescence study of uPAR internalization in uPA–PAI-1 challenged LB6 clone 19 cells. Untreated or cycloheximide (20 μg/ml, 30 min) treated LB6 clone 19 cells were incubated with uPA or uPA–PAI-1 under various conditions, and then probed with 15 μg/ml R2 anti-uPAR antibody followed by a 1:200 dilution of rhodamine-conjugated secondary anti–mouse antibody (see Materials and Methods). When present, cycloheximide was present throughout the experiment. Negative control included the omission of the specific antibody and showed no staining. (*a*) Incubation with 1 nM uPA for 120 min at 4°C; (*b* and *c*) Incubation with 1 nM uPA–PAI-1 for 120 min at 4°C in the presence of cycloheximide; (*d*) incubation with 1 nM uPA–PAI-1, 120 min at 4°C; (*e* and *f*) incubation with 1 nM uPA–PAI-1, 120 min at 4°C, and then chased for 30 min at 37°C; (*g*) incubation with 1 nM uPA–PAI-1 in the presence of cycloheximide, 120 min at 4°C, and then 30 min chase at 37°C; (*h*) incubation with 1 nM uPA–PAI-1, 120 min at 4°C, and then 30 min at 37°C, in the presence of cycloheximide and 200 nM RAP. Bar, 15 μm.

Figure 5. Effect of cycloheximide on the internalization and degradation of uPA–PAI-1. LB6 clone 19 cells (0.2 × 10^6/well) were incubated with 100,000 cpm ^{125}I-uPA–PAI-1 (1 nM, 7.7 × 10^3 cpm/ng) on ice for 120 min, washed, and then warmed up to 37°C for 0, 30, and 120 min. Acid washed ligand (*circles*), cell-associated (i.e., remaining radioactivity after acid washing) (*squares*) and trichloroacetic acid–soluble ligand in the supernatant (*triangles*) were determined (see Materials and Methods) and the values expressed in percent of bound radioactivity. When present (*closed symbols*) cycloheximide (20 μg/ml) was added 30 min before the binding step and remained in the incubation mixture throughout the experiment. Nonspecific binding was determined by competition with 100 nM pro-uPA and substracted. Bound radioactivity at 4°C was 18.7 and 19.4 fmol/well in the absence or in the presence of cycloheximide, respectively. The amount of degraded uPA–PAI-1 complexes did not change in the presence of cycloheximide (14.4 vs 11.9 fmol in control and cycloheximide-treated cells, respectively). Results are the average of two independent experiments in duplicate (less than 10% variation).
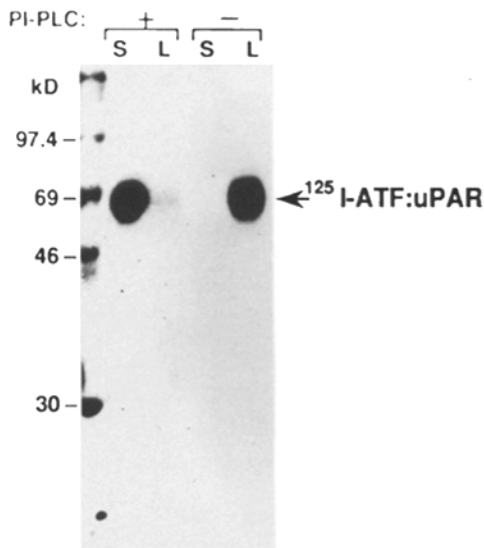
Figure 6. In the absence of ligand essentially all uPAR in LB6 clone 19 cells is surface exposed. LB6 clone 19 cells (0.2×10^6/well) were incubated in the absence or in the presence of PI-PLC (10 U/ml) for 15 min at 37°C, washed and lysed in 1% Triton X-100 lysis buffer (see Materials and Methods). Supernatants (S) and extracts (L) were assayed for solubilized uPAR by cross-linking to ^{125}I-ATF and analyzed by SDS-PAGE and autoradiography (see Materials and Methods section). The conjugate ^{125}I-ATF–uPAR and free ^{125}I-ATF migrate with an apparent mobility of around 70 kD and 15 kD, respectively. Free ^{125}I-ATF has run out of the gel. The migration of molecular weight standards is shown on the left.

degradation. As shown in Fig. 5, the treatment with the protein synthesis inhibitor before and during the incubation at 37°C with uPA–PAI-1, did not affect the uptake parameters: neither the level of acid-wash resistant radioactivity nor the extent of degradation of the uPA–PAI-1 complex. At the concentration used (20 μg/mL) cyclohex-imide inhibited protein synthesis by more than 99% (not shown). When the confocal experiment of Fig. 4 was performed in the presence of cycloheximide, the perinuclear location of uPAR after the 37° incubation was not affected (Fig. 4, e and f). Cycloheximide had also no effect on uPAR distribution at 4° (Fig. 4, b and c). Thus, the perinuclear staining was not due to de novo synthesized uPAR. In conclusion, cycloheximide affected neither uPA–PAI-1 internalization and degradation (Fig. 5) nor the immuno-localization of uPAR while RAP inhibited uPA–PAI-1 internalization and degradation (see Fig. 2) as well as the perinuclear translocation of uPAR (Fig. 4 g). These results thus further support the conclusion that the perinuclear uPAR represents internalized uPAR and that this internalization requires LRP/α_2-MR.

To eliminate the possibility of the presence of a significant intracellular pool of uPAR, we performed an additional experiment testing in the absence of any ligand whether all of the ATF-binding uPAR was exposed on the cell surface in LB6 clone 19 cells. Cells were treated (or not) with PI-PLC and subsequently both the supernatant and the extract were assayed for uPAR by ^{125}I-ATF cross-linking. It is known that under these conditions, cell surface uPAR is released into the supernatant, whereas any

uPAR not present on the cell surface remains in the cell pellet (Møller et al., 1993). Moreover, any immature, biosynthetic uPAR displays a faster migration on gel and can be distinguished from the mature, cell surface form as being completely glycosylated and cell surface exposed (Behrendt et al., 1990; Møller et al., 1992). As shown in Fig. 6, in the absence of the PI-PLC treatment, most (over 95% as judged by film scanning) of uPAR was present in the cell lysate, as shown by the presence of the ∼70 kD ^{125}I-ATF–uPAR conjugate, whereas after a treatment with PI-PLC, all of it was present in the supernatant. Moreover, the migration of the ATF-uPAR adduct was identical in the two conditions. This experiment shows therefore the absence of any major intracellular pool of uPAR within LB6 clone 19 cells.

Internalization of uPAR was also followed by electron microscopy of cryosections prepared for immunocytochemistry, using LB6 clone 19 cells incubated and prepared as described in the Materials and Methods section. After incubation for 2 h at 0°C with 100 nM uPA–PAI-1, 77% uPAR was found located on the plasma membrane including microvilli, whereas only 23% was found in intracellular vacuoles (Fig. 7, A and B and Table I). However, after further chase incubation at 37° for 30 min, the labeling of the plasma membrane decreased from 77 to 7% and the intracellular vacuolar labeling increased from 23 to 93% mainly along the endosomal membrane (Fig. 8, A–D and Table I). Identical results were obtained with affinity-purified polyclonal as well as monoclonal anti-uPAR antibodies. Internalization was totally abolished if the cells were incubated under the same conditions but with the addition of 400 nM RAP (Fig. 9 A and Table I). Likewise, there was no internalization of uPAR if the cells were incubated under the same conditions but using DFP-uPA instead of uPA–PAI-1 (Fig. 9 B and Table I). In conclusion, we show that plasma membrane uPAR can be translocated into intracellular endosome-like particles, but this process is specific for uPA–PAI-1, occurs only at 37°C and is inhibited by the LRP/α_2MR agonist RAP.

Discussion

The receptor for uPA has the peculiar property of inducing the internalization of some (uPA-serpin complexes) but not other ligands (uPA, pro-uPA, DFP-uPA, ATF) (Cubellis et al., 1990). This property is acquired because the serpin moiety can interact with the LRP/α_2-MR or other members of the LDL receptor gene family (Nykjær et al., 1992; Herz et al., 1992; Moestrup et al., 1993a; Kounnas et al., 1993; Li et al., 1994). Previous studies have shown that uPAR binding represents the first and essential step for an efficient degradation of uPA–serpin complexes in human U937 cells and in murine LB6 clone 19 cells (Olson et al., 1992; Conese et al., 1994). Indeed, at physiological concentrations, only serpin complexes with uPA derivatives containing the uPAR-binding region (i.e., solely two-chain uPA) can be degraded, while those missing the growth factor domain (33 kD, low molecular weight-uPA, 33-kD-uPA–PAI-1 or 33-kD-uPA–PN-1 complexes) cannot (Vassalli et al., 1985; Stoppelli et al., 1985, 1986; Cubellis et al., 1986, 1990; Jensen et al., 1990; Olson et al., 1992; Conese et al., 1994). Moreover, complexes of the same serpin with other
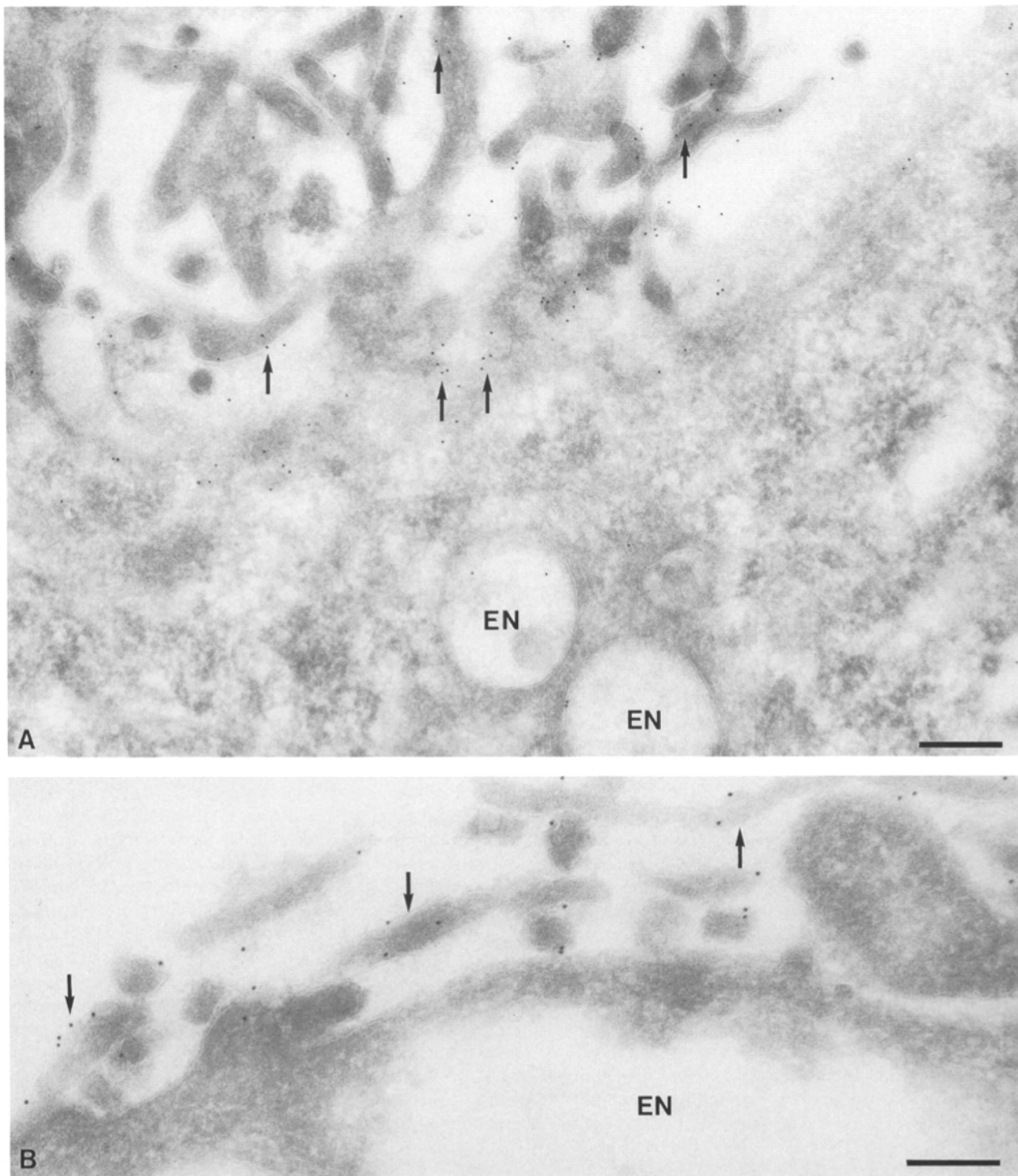
Figure 7. Immuno-electron microscopy analysis of uPAR internalization in LB6 clone 19 cells: incubation with uPA–PAI-1 at 0°C. Electron micrographs from cryosections of LB6 clone 19 cells were prepared for immunocytochemistry as described in the Materials and Methods section. The cells were incubated with 100 nM uPA–PAI-1 for 3 h at 0°C, washed, and fixed. (*A*) Polyclonal rabbit affinity-purified anti-uPAR antibodies. (*B*) Mouse monoclonal anti-uPAR antibody R2. Labeling is seen on the plasma membrane including microvilli (*arrows*). Endosomes (EN) show very little labeling. Bars, 0.25 μm.

proteases (like the thrombin:PN-1 complex) fail to compete for uPA–PN-1 degradation (Conese et al., 1994). Finally, prevention of binding to uPAR by specific uPAR antibodies, nondegradable uPA derivatives (like ATF, DFP-uPA) or by treatment of cells with the uPAR-releas-

ing PI-PLC, prevents internalization and degradation of uPA-serpin complexes (Olson et al., 1992; Conese et al., 1994).

On the other hand, the LRP/α$_2$-MR ligand RAP and LRP/α$_2$-MR antibodies, while incapable of preventing cell

binding, do inhibit degradation and internalization of the uPA–serpin complexes (Nykjær et al., 1992; Conese et al., 1994). Since uPA–serpins can bind LRP/α_2-MR (Fig. 1), as already shown previously (Kounnas et al., 1993; Nykjær et al., 1992, 1994a; Conese et al., 1994), we believe that binding initially to uPAR and subsequently to LRP/α_2-MR are prerequisites for internalization and degradation. Because of their affinity for LRP/α_2-MR, high concentrations of uPA–serpin complexes may still be taken up in uPAR-lacking cells, and in this case the uptake is enhanced by the transfection of uPAR cDNA (Li et al., 1994).

Uptake of the uPA–PAI-1 complex into lysosomes (Jensen et al., 1990; Olson et al., 1992) is followed by its degradation (Cubellis et al., 1990). The mechanism underlying uPA–serpin internalization and the respective functions of uPAR and LRP/α_2-MR are issues that are not yet clear. With cells containing both receptors and when the ligands are used at physiological concentrations, uPAR is clearly the binding site, in agreement with the measured affinities of uPA–PAI-1 for uPAR and LRP/α_2-MR (Cubellis et al., 1989; Nykjær et al., 1994). At higher concentrations, LRP/α_2-MR might directly bind to and hence internalize uPA–serpins even in the absence of uPAR (Kounnas et al., 1993; Nykjær et al., 1994a).

Downregulation of uPAR during uPA–PAI-1 internalization has been suggested previously (Olson et al., 1992; Li et al., 1994). We now demonstrate that downregulation coincides with the internalization of uPAR (Figs. 3, 4, 5, and 7–9). Moreover, both uPAR downregulation in cytofluorimetry (Fig. 3) and internalization by confocal immunofluorescence and immunoelectron microscopy experiments (Figs. 4, 7–9) are LRP/α_2-MR–dependent, as demonstrated by the inhibitory effect of RAP. The confocal data suggest a translocation of uPAR from the pericellular to a perinuclear position only when cells have been exposed to the uPA–serpin complex and after they have been incubated at 37°C. Computer reconstruction images do show that under those conditions the interior of the cell is filled with uPAR (not shown).

The immunoelectron microscopy experiments of Figs. 7–9, carried out under conditions in which uPAR was saturated by the ligand, demonstrate the internalization of uPAR. When cells were analyzed in the absence of ligands (not shown) or in the presence of uPA–PAI-1 at 0°C (Fig. 7, A and B), uPAR was observed exclusively at the cell surface or on microvilli, in agreement with the internalization specificity for the uPA–serpin complexes. In particular, endosome-like structures were largely deprived of specific labeling. When, however, cells exposed to uPA–PAI-1 complex were further chased at 37°C, uPAR was also found in vacuolar, endosome-like structures (Fig. 8, A–D). The presence of intracellular uPAR was no longer observed when the incubation mixture also contained the LRP/α_2MR agonist, RAP (Fig. 9 A).The internalization of uPAR was specific for the uPA–PAI-1 complex; in fact, with DFP-uPA at 37°C (Fig. 9 B), the electron microscopy experiment gave results identical to those observed with uPA–PAI-1 only incubated at 0°C. That the vacuolar structures did not represent invaginations of the plasma membrane is strongly suggested by the very appearance of the vesicles and by the following evidence: (a) LB6 clone 19 cells, as opposed to other cells (i.e., human monocytes), have a quite regular

surface with no deep invaginations (data not shown). (b) The size of the vesicle was ~0.7 μm in diameter, and the distance from the plasma membrane often ~2.5 μm.

The quantitative analysis of the electron microscopy experiments unequivocally demonstrates the internalization of uPAR. In fact (Table I), uPAR translocation from the plasma membrane to intracellular vacuoles appeared to be quantitative (over 90%), specific (not observed with DFP-uPA), and dependent on the LRP/α_2MR agonist (inhibited by RAP).

That intracellular uPAR does not represent biosynthetic uPAR nor an intracellular pool of uPAR is shown by the lack of effect of the protein synthesis inhibitor cycloheximide (as tested in uPA–PAI-1 degradation and in uPAR confocal microscopy experiments) and by the lack of an intracellular pool of uPAR in the absence of ligands, as studied by cross-linking experiments (Figs. 4–6). On the other hand, the dependence of uPAR downregulation by the LRP/α_2-MR was confirmed also in the cytofluorimetry and confocal and electron microscopy experiments (Figs. 3, 4, and 9).

On the basis of the results presented in this paper, we conclude that during the process of the internalization of the uPA–serpins, uPAR itself is internalized. This process is tied up with that of LRP/α_2-MR, but we do not know whether a tripartite uPAR/uPA–serpin/LRP/α_2-MR complex is internalized as a whole, or through different pathways. The situation is complicated by the fact that uPAR is GPI-anchored and might therefore also be located in areas, like caveolae, distinct from those accessible to LRP/α_2-MR. However, a recombinant uPAR molecule anchored via a transmembrane region internalizes uPA–PAI-1 complexes as efficiently as the GPI-anchored uPAR in LRP/α_2-MR–expressing cells (Li et al., 1994; Møller, L. B., and F. Blasi, unpublished results).

The results presented in this paper demonstrate therefore that the process of uPA–PAI-1 internalization is complex. Such a mechanism must be common to the internalization of both uPA–PAI-1 and uPA–PN-1 as the kinetics and the dependence on LRP/α_2-MR are the same. The fate of uPAR after internalization remains an open question. One possibility is that it may be delivered to the lysosomes and degraded. Alternatively, uPAR might be recy-

Table I. Distribution of uPAR on LB6 Clone 19 Cells As Determined by Electron Microscope Immunocytochemistry

	uPA–PAI-1[‡] 0 min	uPA–PAI-1[‡] 30 min	uPA–PAI-1/RAP[‡] 30 min	DFP-uPA[‡] 30 min
	%	%	%	%
Plasma membrane	76.9	7.0	79.7	82.4
Cytoplasmin vacuoles	23.1	93.0	20.3	17.6
Total number of gold particles counted	1,540	840	2,149	3,620

*Grain counting is outlined in detail in the Materials and Methods section. The data are shown as % of total grains, and the number of grains counted is shown in the last row of each column.
‡These columns indicate the four incubation conditions outlined in detail in the Materials and Methods section. In particular, here they denote the ligand and effector with which the cells were incubated at 0°C, and the time of chase at 37°C.
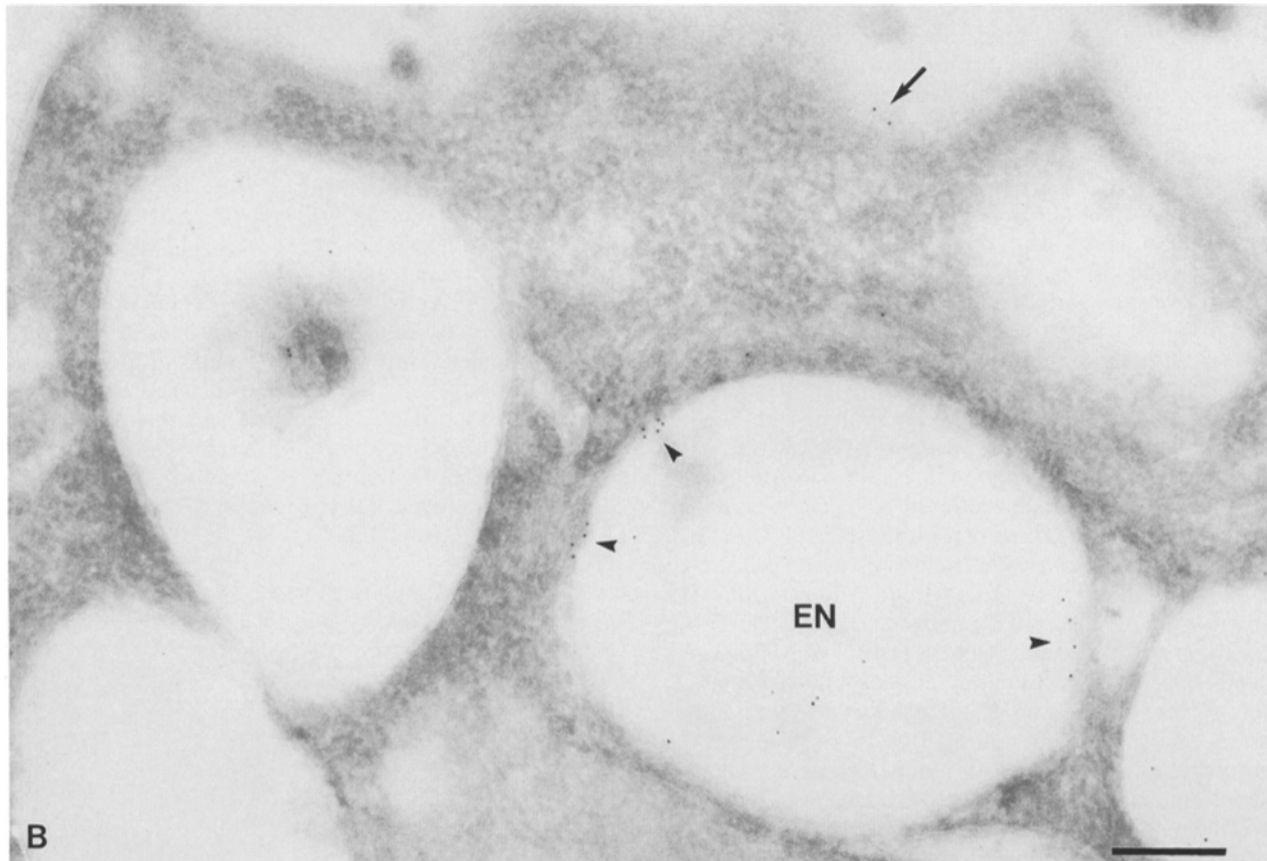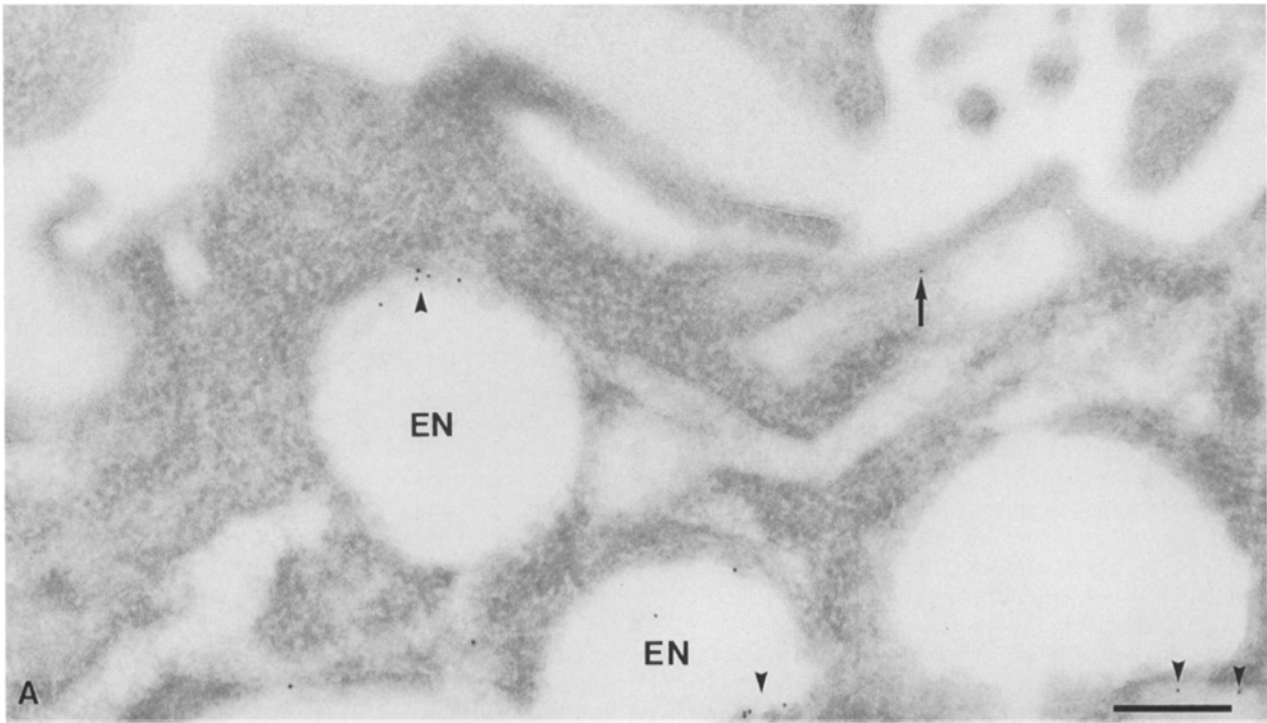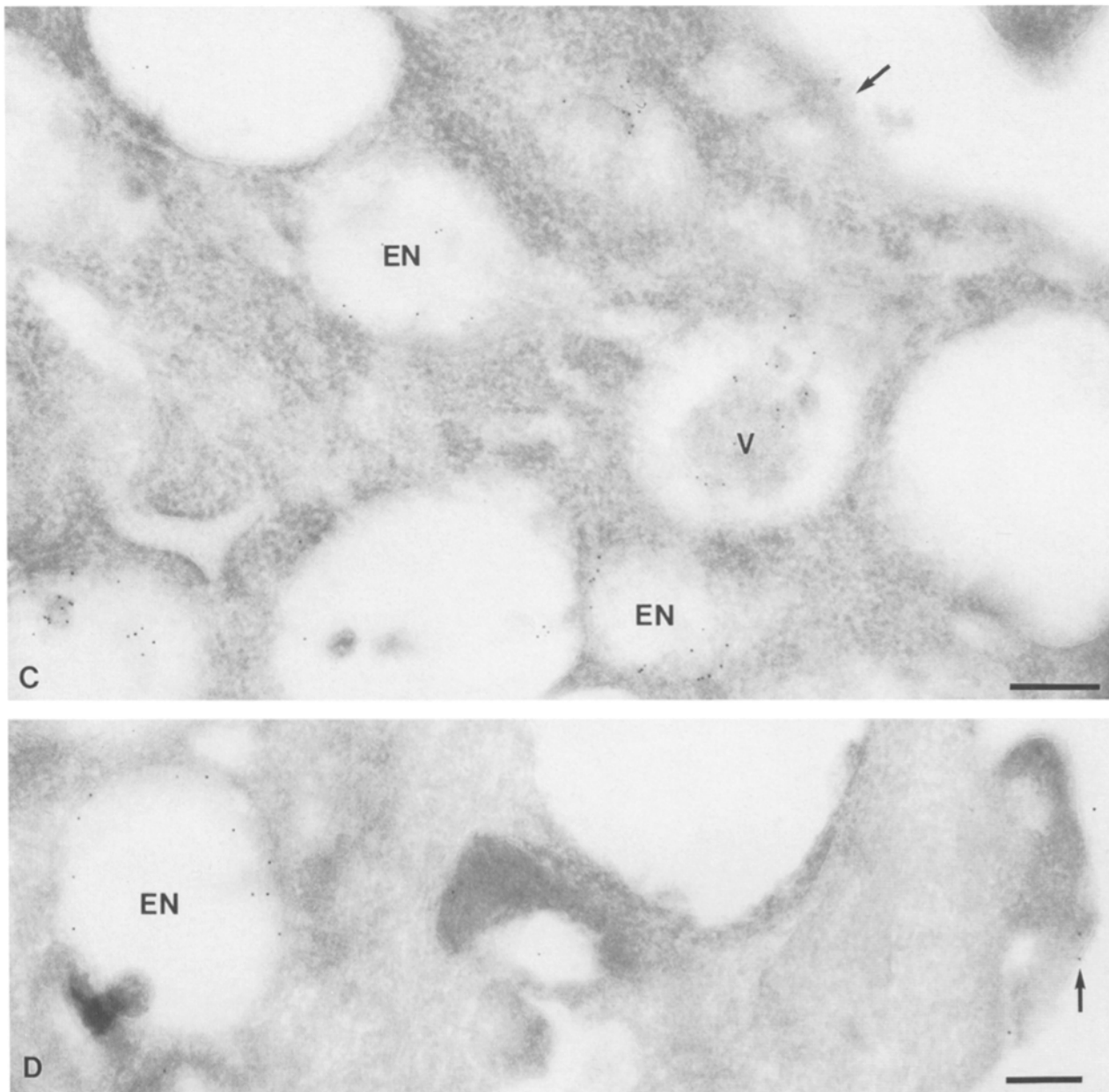
Figure 8. Immuno-electron microscopy analysis of uPAR internalization in LB6 clone 19 cells: incubation with uPA–PAI-1 at 0°C with further chase at 37°C. Cells were incubated with uPA–PAI-1 as in Fig. 7 *A,* and then chased for 30 min at 37°C. *(A–C)* Polyclonal rabbit affinity purified anti-uPAR antibody. *(D)* Mouse monoclonal antibody R2. Only little labeling is left on the plasma membrane *(arrows)*; however, significant labeling is seen in endosomes (EN), mainly along the endosomal membrane *(arrowheads)* but occasionally also over electron-dense material in cytoplasmic vacuoles (V). In *D,* the use of the monoclonal antibody gives results identical to the polyclonal antibody, demonstrating labeling of the membrane of an endosome (EN) located deep in the cytoplasm and only a few gold particles on the plasma membrane. Bars, 0.25 μm.

cled back to the cell surface. Recycling of uPAR would be consistent with a mechanism stimulating extracellular proteolysis and cell migration by continuously modifying the geographic location of the surface areas capable of binding active uPA, focally forming plasmin and hence cleaving proteins at cell–matrix or cell–cell contacts. These continuous modifications would be triggered and regulated by the formation of the uPA–serpin complexes, since both PAI-1 and PN-1 are present in the extracellular matrix. In particular, active PAI-1 is directly bound by the extracellular matrix protein vitronectin (Salonen et al., 1989). The recent report that uPAR can bind, in addition to uPA, also vitronectin (Wei et al., 1994), would be in agreement with the above hypothesis, as the binding of vitronectin to uPAR would allow direct regulation of cell surface uPA activity. This hypothesis would also explain the apparent paradox that increase in PAI-1 is associated with a higher metastatic risk in human cancer (Grøndahl-Hansen et al., 1993). We are currently investigating whether uPAR in fact undergoes recycling after internalization.
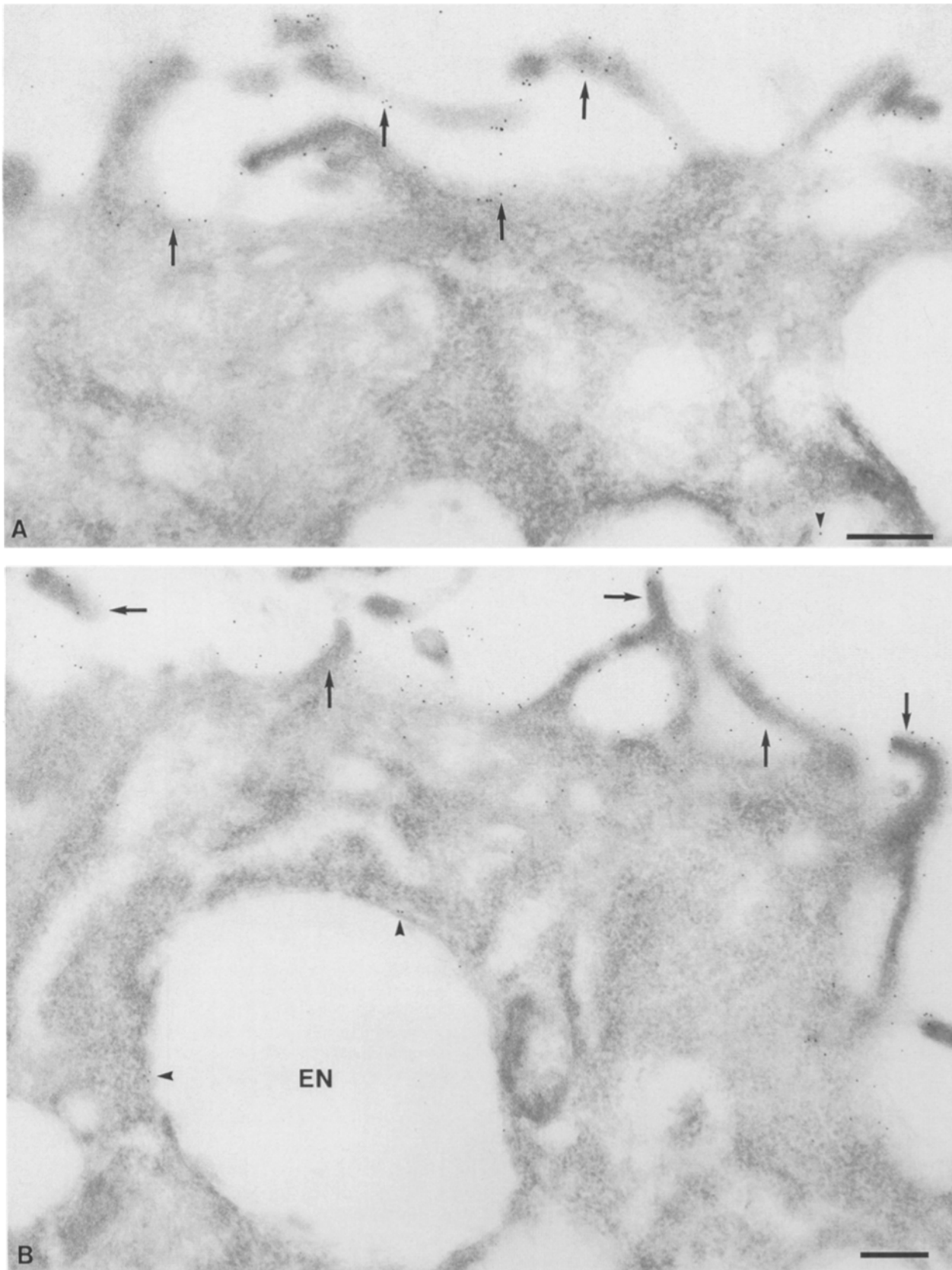
Figure 9. Immuno-electron microscopy analysis of uPAR internalization in LB6 clone 19 cells: dependence on LRP/α₂MR and specificity for uPA–PAI-1. (*A*) Cells were incubated as in Fig. 8, but with the addition of 400 nM RAP. (*B*) Cells were preincubated for 2 h with 100 nM DFP-uPA at 0°C, and then chased for 30 min at 37°C. In both cases the antibody was rabbit anti-uPAR serum, affinity-purified. (*A*)In these cells the plasma membrane is heavily labeled including the microvilli (*arrows*) and only occasional labeling of endosomes is seen (*arrowheads*), showing the requirement for LRP/α₂MR. (*B*) Again, the plasma membrane and the microvilli are heavily labeled and only little endosomal labeling is seen (EN, *arrowheads*), in agreement with the deficient internalization of DFP-uPA. Bars, 0.25 μm.

The internalization process might also be connected with uPAR-mediated signal transduction. Indeed, in the presence of a chemotactic gradient, uPAR has been shown to cluster at the leading edge of monocytic cells (Eistrecher et al., 1990; Gyetko et al., 1994). Moreover, it has been shown that several protein molecules, including non-receptor tyrosine kinases and integrins, are present in a macromolecular complex containing uPAR (Bohuslav et al., 1995). However, we have no information as to how these findings relate to known functions of uPAR, nor to its LRP/α_2MR-mediated internalization. Additional work is needed to clarify all these points.

References

Appella, E., E. A. Robinson, S. J. Ulrich, M. P. Stoppelli, A. Corti, G. Cassani, and F. Blasi. 1987. The receptor-binding sequence of urokinase. A biological function for the growth-factor module of proteases. *J. Biol. Chem.* 262: 4437–4440.

Ashcom, J. D., S. E. Tiller, K. Dickerson, J. L. Cravens, W. S. Argraves, and D. K. Strickland. 1990. The human α_2-macroglobulin receptor: identification of a 420-kD cell surface glycoprotein specific for the activated conformation of α_2-macroglobulin. *J. Cell Biol.* 110:1041–1048.

Behrendt, B., E. Rønne, M. Ploug, T. Petri, D. Løber, L.S. Nielsen, W.-D. Schleuning, F. Blasi, E. Appella, and K. Danø. 1990. The human receptor for urokinase plasminogen activator. NH$_2$-terminal amino acid sequence and glycosylation variants. *J. Biol. Chem.* 265:6453–6460.

Bergman, B., R. Scott, A. Bajpai, A. Watts, and J. Baker. 1986. Inhibition of tumor-cell-mediated extracellular matrix destruction by a fibroblast proteinase inhibitor, protease nexin I. *Proc. Natl. Acad. Sci. USA.* 83:996–1000.

Biesegel, U., W. Weber, and G. Bengtsson-Olivecrona. 1991. Lipoprotein lipase enhances the binding of chylomicrons to low density lipoprotein receptor-related protein. *Proc. Natl. Acad. Sci. USA.* 88:8342–8346.

Bohuslav, J., V. Horejsì, C. Hansmann, J. Stöck, U.H. Weidle, O. Majdic, I. Bartke, W. Knapp, and H. Stockinger. 1995. Urokinase plasminogen activator receptor, β-2 integrins and Src-kinases within a single receptor complex of human monocytes. *J. Exp. Med.* 181:1381–1390.

Conese, M., D. Olson, and F. Blasi. 1994. Protease nexin-1-urokinase complexes are internalized and degraded through a mechanism that requires both urokinase receptor and α_2-macroglobulin receptor. *J. Biol. Chem.* 269: 17886–17892.

Conese, M., U. Cavallaro, N. Sidenius, D. Olson, M. R. Soria, and F. Blasi. 1995. PMA-induced down regulation of the receptor for α_2-macroglobulin in human U937 cells. *FEBS Lett.* 358:73–78.

Crowley, C. W., R. L. Cohen, B. K. Lucas, G. Liu, M. A. Shuman, and A. D. Levinson. 1993. Prevention of metastasis by inhibition of the urokinase receptor. *Proc. Natl. Acad. Sci. USA.* 90:5021–5025.

Cubellis, M. V., M. L. Nolli, G. Cassani, and F. Blasi. 1986. Binding of single-chain prourokinase to the urokinase receptors on human U937 cells. *J. Biol. Chem.* 261:15819–15822.

Cubellis, M. V., T.-C. Wun, and F. Blasi. 1990. Receptor-mediated internalization and degradation of urokinase is caused by its specific inhibitor PAI-1. *EMBO (Eur. Mol. Biol. Organ.) J.* 9:1079–1085.

Cubellis, M.V., P. A. Andreasen, P. Ragno, M. Mayer, K. Danø, and F. Blasi. 1989. Accessibility of receptor-bound urokinase to type-1 plasminogen activator inhibitor. *Proc. Natl. Acad. Sci. USA.* 86:4828–4832.

Ellis, V., M. F. Scully, and V. V. Kakkar. 1989. Plasminogen activation initiated by single-chain urokinase-type plasminogen activator. *J. Biol. Chem.* 264: 2185–2188.

Estreicher, A., J. Mulhauser, J.-L. Carpentier, L. Orci, and J.-D. Vassalli. 1990. The receptor for urokinase type plasminogen activator polarizes expression of the protease to the leading edge of migrating monocytes and promotes degradation of enzyme inhibitor complexes. *J. Cell Biol.* 111:783–792.

Fazioli, F., and F. Blasi. 1994. Urokinase-type plasminogen activator and its re-

ceptor: new targets for anti-metastatic therapy? *Trend. Pharmacol. Sci.* 15: 25–29.

Griffiths, G., A. McDowall, R. Back, and J. Dubochet. 1984. On the preparation of cryosections for immunocytochemistry. *J. Ultrastruct. Res.* 89:65–78.

Grøndahl-Hansen, J., I. J. Christensen, C. Rosenquist, N. Brünner, H. T. Mouridsen, K. Danø, and M. Blicher-Toft. 1993. High levels of urokinase-type plasminogen activator (uPA) and its inhibitor PAI-1 in cytosolic extracts of breast carcinomas are associated with poor prognosis. *Cancer Res.* 53:2513–2521.

Gyetko, M. R., R. F. Todd III, C. C. Wilkinson, and R. G. Sitrin. 1994. The urokinase receptor is required for human monocyte chemotaxis in vitro. *J. Clin. Invest.* 93:1380–1387.

Hearing, V., L. Law, A. Corti, E., Appella, and F. Blasi. 1988. Modulation of metastatic potential by cell surface urokinase of murine cells. *Cancer Res.* 48: 1270–1278.

Herz, J., D. E. Clouthier, and R. E. Hammer. 1992. LDL-receptor-related protein internalizes and degrades uPA-PAI-1 and is essential for embryo implantation. *Cell.* 71:411–421.

Holmberg, L., B. Bladh, and B. Astedt. 1976. Purification of urokinase by affinity chromatography. *Biochim. Biophys. Acta.* 445:215–222.

Hopkins, C. R., A. Gibson, M. Shipman, D. K. Strickland, and I. S. Trowbridge. 1994. In migrating fibroblasts, recycling receptors are concentrated in narrow tubules in the pericentriolar area, and then routed to the plasma membrane of the leading lamella. *J. Cell Biol.* 125:1265–1274.

Huber, R., and R. W. Carrell. 1989. Implications of the three-dimensional structure of α_1-antitrypsin for structure and function of serpins. *Biochemistry.* 28: 8951–8966.

Jensen, P. H., S. K. Moestrup, and J. Gliemann. 1989. Purification of the human placental α_2-macroglobulin receptor. *FEBS Lett.* 255:275–280.

Jensen, P. H., E. I.Christensen, P. Ebbesen, J. Gliemann, and P. A. Andreasen. 1990. Lysosomal degradation of receptor-bound urokinase-type plasminogen activator is enhanced by its inhibitors in human trophoblastic choriocarcinoma cells. *Cell Regulation.* 1:1043–1056.

Kirchheimer, J. C., and H. G. Remold. 1989. Functional characteristics of receptor-bound urokinase on human monocytes: catalytic efficiency and susceptibility to inactivation by plasminogen activator inhibitors. *Blood.* 74: 1396–1402.

Kobayashi, H., J. Gotoh, M. Fujie, H. Shinohara, N. Moniwa, and T. Terao. 1994. Inhibition of metastasis of Lewis lung carcinoma by a synthetic peptide within growth factor-like domain of urokinase in the experimental and spontaneous metastasis model. *Int. J. Cancer.* 57:723–733.

Kook, Y. H., J. Adamski, A. Zelent, and L. Ossowski. 1994. The effect of antisense inhibition of urokinase receptor in human squamous cell carcinoma on malignancy. *EMBO(Eur. Mol. Biol. Organ.) J.* 13:3983–3991.

Kounnas, M. Z., R. Morris, M. Thompson, D. FitzGerald, D. Strickland, and C. Saelinger. 1992. The α_2-macroglobulin receptor/low density lipoprotein receptor-related protein binds and internalizes *Pseudomonas* exotoxin A. *J. Biol. Chem.* 267:12420–12423.

Kounnas, M., J. Henkin, W. S. Argraves, and D. K. Strickland. 1993. Low density lipoprotein receptor-related protein/α_2-macroglobin receptor mediates cellular uptake of pro-urokinase. *J. Biol. Chem.* 268:21862–21867.

Kowal, R. C., J. Herz, K. H.Weisgraber, R. W. Mahley, M. S. Brown, and J. L. Goldstein. 1990. Opposing effects of apolipoproteins E and C on lipoprotein binding to low density lipoprotein receptor-related protein. *J. Biol. Chem.* 265:10771–10779.

Laemmli, U. K. 1970. Cleavage of structural proteins during the assembly of the head of bacteriophage T4. *Nature(Lond.).* 227:680–685.

Li, H., A. Kuo, J. Kochan, D. Strickland, K. Kariko, E. S. Barnathan, and D. B. Cines. 1994. Endocytosis of urokinase plasminogen activator inhibitor type 1 complexes bound to a chimeric transmembrane urokinase receptor. *J. Biol. Chem.* 269:8153–8158.

Moestrup, S. K., and J. Gliemann, 1991. Analysis of ligand recognition by the purified α_2-macroglobulin receptor (low density lipoprotein receptor-related protein). Evidence that high affinity of α_2-macroglobulin-proteinase complex is achieved by binding to adjacent receptors. *J. Biol. Chem.* 266:14011–14017.

Moestrup, S. K., K. Kaltoft, L. Sottrup-Jensen, and J. Gliemann. 1990. The human α_2-macroglobulin receptor contains high affinity calcium binding sites important for receptor conformation and ligand recognition. *J. Biol. Chem.* 265:12623–12628.

Moestrup, S. K., S. Nielsen, P. Andreasen, K. E. Jørgensen, A. Nykær, H. Røigaard, J. Gliemann, and E. I. Christensen. 1993a. Epithelial glycoprotein-330 mediates endocytosis of plasminogen activator-plasminogen activator inhibitor type-1 complexes. *J. Biol. Chem.* 268:16564–16570.

Moestrup, S. K., T. L. Holtet, M. Etzerodt, H. C. Thøgersen, A. Nykær, P. A. Andreasen, H. H. Rasmussen, L. Sottrup-Jensen, and J. Gliemann. 1993b. α_2-macroglobulin-proteinase complexes, plasminogen activator inhibitor type-1-plasminogen activator complexes, and receptor-associated protein bind to a region of the α_2-macroglobulin receptor containing a cluster of eight complement-type repeats. *J. Biol. Chem.* 268:13691–13696.

Møller, L. B., M. Ploug, and F. Blasi. 1992. Structural requirements for glycosyl-phosphatidylinositol anchor attachment in the cellular receptor for urokinase plasminogen activator. *Eur. J. Biochem.* 208:493–500.

Møller, L. B., J. Pöllänen, E. Rønne, N. Pedersen, and F. Blasi. 1993. N-linked glycosylation of the ligand binding domain of the human urokinase receptor

contributes to the affinity for its ligand. *J. Biol. Chem.* 268:11152–11159.

Nykjær, A., C. M. Petersen, E. I. Christensen, O. Davidsen, and J. Gliemann. 1990. Urokinase receptors in human monocytes. *Biochim. Biophys. Acta.* 1052:399–407.

Nykjær, A., C. M. Petersen, B. Møller, P. H. Jensen, S. K. Moestrup, T. L. Holtet, M. Etzerodt, H. C. Thøgersen, M. Munch, P. A. Andreasen, et al. 1992. Purified α_2 macroglobulin receptor/LDL receptor related protein binds urokinase-plasminogen activator inhibitor type-1 complex. Evidence that α_2 macroglobulin receptor mediates cellular degradation of urokinase receptor-bound complexes. *J. Biol. Chem.* 267:14543–14546.

Nykjær, A, L. Kjøller, R. L. Cohen, D. A. Lawrence, B. A. Garni-Wagner, R. F. Todd III, A.-J. van Zonneveld, J. Gliemann, and P. A. Andreasen. 1994a. Binding of urokinase:type-1 inhibitor complex and pro-uPA to the endocytic α_2-macroglobulin receptor/LDL receptor-related protein involves multiple independent contacts between ligands and receptor. Evidence that the urokinase receptor protects pro-urokinase against binding to the endocytic receptor. *J. Biol. Chem.* 269:25668–25676.

Nykjær, A., M. S. Nielsen, N. Meyer, H. Røigaard, M. Etzerodt, A. Lookene, U. Beisiegel, G. Olivecrona, and J. Gliemann. 1994b. A C-terminal fragment of lipoprotein lipase binds to LDL receptor-related protein and inhibits the lipase mediated uptake of lipoprotein in cells. *J. Biol. Chem.* 269:31747–31755.

Olson, D., J. Pöllänen, G. Høyer-Hansen, E. Rønne, K. Sakaguchi, T.-C. Wun, E. Appella, K. Danø, and F. Blasi. 1992. Internalization of the urokinase: plasminogen activator inhibitor type 1 complex is mediated by the urokinase receptor. *J. Biol. Chem.* 267:9129–9133.

Orth, K., E. L. Madison, M.-J. Gething, J. F. Sambrook, and J. Herz. 1992. Complexes of tissue-type plasminogen activator and its serpin inhibitor plasminogen-activator inhibitor type 1 are internalized by means of the low density lipoprotein receptor-related protein/α_2-macroglobulin receptor. *Proc. Natl. Acad. Sci. USA.* 89:7422–7426.

Ossowski, L. 1988. In vivo invasion of modified chorioallantoic membrane by tumor cells: the role of cell-surface bound urokinase. *J. Cell Biol.* 107:2437–2445.

Ossowski, L., and E. Reich. 1983. Antibodies to plasminogen activator inhibit human tumor metastasis. *Cell.* 52:321–328.

Ossowski, L., G. Clunie, M. T. Masucci, and F. Blasi. 1991. In vivo interaction between urokinase and its receptor: effect on tumor cell invasion. *J. Cell Biol.* 115:1107–1112.

Picone, R., E. L. Kajtaniak, L. S. Nielsen, N. Behrendt, M. R. Mastronicola, M. V. Cubellis, M. P. Stoppelli, S. Pedersen, K. Danø, and F. Blasi. 1989. Regulation of urokinase receptors in monocyte-like U937 cells by phorbol ester phorbol myristate acetate. *J. Cell Biol.* 108:693–702.

Plough, M., E. Rønne, N. Behrendt, A. L. Jensen, F. Blasi, and K. Danø. 1991. Cellular receptor for urokinase plasminogen activator: carboxy-terminal processing and membrane anchoring by glycosyl-phosphatidylinositol. *J.*

Biol. Chem. 266:1926–1933.

Potempa, J., E. Korzus, and J. Travis. 1994. The serpin superfamily of proteinase inhibitors: structure, function, and regulation. *J. Biol. Chem.* 269:15957–15960.

Quax, P. H. A., N. Pedersen, M. T. Masucci, E. J. D. Weening-Verhoeff, K. Danø, J. H. Verheijen, and F. Blasi. 1991. Complementation analysis of extracellular matrix degradation: enhancement of urokinase plasminogen activation by the urokinase receptor. *Cell Regulation.* 2:793–803.

Roldan, A. L., M. V. Cubellis, M. T. Masucci, N. Behrendt, L. R. Lund, K. Danø, and F. Blasi. 1990. Cloning and expression of the receptor for human urokinase plasminogen activator, a central molecule in cell-surface plasmin-dependent proteolysis. *EMBO (Eur. Mol. Biol. Organ.) J.* 9:467–474.

Rønne, E., N. Behrendt, V. Ellis, M. Ploug, K. Danø, and G. Høyer-Hansen. 1991. Cell induced potentiation of the plasminogen activation system is abolished by a monoclonal antibody that recognizes the NH_2-terminal domain of the urokinase receptor. *FEBS Lett.* 288:233–236.

Salonen, E.-M., A. Vaheri, J. Pöllänen, R. Stephens, P. Andreasen, M. Mayer, K. Danø, J. Gailit, and E. Ruoshlati. 1989. Interaction of plasminogen activator inhibitor (PAI-1) with vitronectin. *J. Biol. Chem.* 264:6339–6343.

Sherman, P. M., D. A. Lawrence, A.Y. Yang, E.T. Vanderberg, D. Paielli, S. T. Olson, J. D. Shore, and D. Ginsburg. 1992. Saturation mutagenesis of the plasminogen activator inhibitor-1 reactive center. *J. Biol. Chem.* 267:7588–7595.

Stoppelli, M. P., A. Corti, A. Soffientini, G. Cassani, F. Blasi, and R. K. Assoian. 1985. Differentiation-enhanced binding of the amino-terminal fragment of human urokinase plasminogen activator to a specific receptor on U937 monocytes. *Proc. Natl. Acad. Sci. USA.* 82:4939–4943.

Stoppelli, M. P., C. Tacchetti, M. V. Cubellis, A. Corti, V. J. Hearing, G. Cassani, E. Appella, and F. Blasi. 1986. Autocrine saturation of pro-urokinase receptors on human A431 cells. *Cell.* 45:675–684.

Strickland, D. K., J. D. Ashcom, S. Williams, F. Battey, E. Behere, K. McTigue, J. F. Battey, and W. S. Argraves. 1991. Primary structure of α_2-macroglobulin receptor-associated protein. Human homologue of a Heymann nephritis antigen. *J. Biol. Chem.* 266:13364–13369.

Tokuyasu, K. T. 1978. A study of positive staining of ultrathin frozen sections. *J. Ultrastruct. Res.* 63:287–307.

Vassalli, J.-D., D. Baccino, and D. Belin. 1985. A cellular binding site for the M_r 55,000 form of the human plasminogen activator, urokinase. *J. Cell Biol.* 100:86–92.

Wei, Y., D. A. Waltz, N. Rao, R. J. Drummond, S. Rosenberg, and H. A. Chapman. 1994. Identification of the urokinase receptor as an adhesion receptor for vitronectin. *J. Biol. Chem.* 269:32380–32388.

Willnow, T. E., J. L. Goldstein, K. Orth, M. S. Brown, and J. Herz. 1992. Low density lipoprotein receptor-related protein and gp330 bind similar ligands, including plasminogen activator-inhibitor complexes and lactoferrin, an inhibitor of chylomicron remnant clearance. *J. Biol. Chem.* 267:26172–26180.